Frequency-Offset Estimation and Correction in a Digital Receiver

From Pulse-Shaped BPSK to Practical SDR Implementation

B. N. Bharath
Department of Electrical, Electronics and Communication Engineering (EECE)
Indian Institute of Technology Dharwad

Abstract

These notes explain how carrier-frequency offset (CFO) appears in a digital communication receiver, how it is represented in complex baseband, and how it is estimated and corrected in the digital domain. The development begins with pulse-shaped BPSK, derives the I/Q baseband CFO model, develops pilot-based and repeated-preamble estimators, and concludes with a practical SDR receiver architecture including numerically controlled oscillators (NCOs), coarse and fine frequency correction, matched filtering, timing recovery, and Costas-loop tracking.

1. Starting Point: Pulse-Shaped BPSK

Consider BPSK symbols $a_k \in \{-1, +1\}$ with symbol duration T_m. Let $p(t)$ be a unit-energy pulse,

$$\int_{-\infty}^{\infty} |p(t)|^2 \, dt = 1.$$

To transmit energy $E_b = PT_m$ per bit, the pulse-shaped baseband waveform is

$$\boxed{x(t) = \sqrt{PT_m} \sum_k a_k p(t - kT_m).}$$

For the isolated kth symbol, $x_k(t) = \sqrt{PT_m}\, a_k p(t - kT_m)$, so

$$\int_{-\infty}^{\infty} |x_k(t)|^2 \, dt = PT_m = E_b.$$

This representation separates the discrete symbol sequence $\{a_k\}$ from the continuous pulse shape $p(t)$. In practice, $p(t)$ is typically chosen as a root-raised-cosine (RRC) pulse and implemented digitally as an FIR filter.

2. Digital Pulse-Shaping Implementation

Let the digital sample interval be T_s, with sample rate $F_s = 1/T_s$. If there are N_s samples per symbol, then

$$\boxed{N_s = \frac{T_m}{T_s}.}$$

The sampled pulse is $p[n] = p(nT_s)$. If $p(t)$ has unit continuous-time energy, the Riemann-sum approximation is

$$\boxed{T_s \sum_n |p[n]|^2 \approx 1.}$$

If the discrete filter taps are explicitly normalized in software, one may instead enforce $\sum_n |p[n]|^2 = 1$; the normalization convention must simply be used consistently.

2.1 Upsampling and RRC FIR filtering

The symbol-rate sequence $a[0], a[1], \ldots$ is upsampled by N_s:

$$a_{\uparrow}[n] = \begin{cases} a_k, & n = kN_s, \\ 0, & \text{otherwise.} \end{cases}$$

The RRC FIR filter then produces

$$\boxed{x[n] = \sqrt{PT_m} \sum_k a_k p[n - kN_s].}$$

This is the sampled version of the continuous-time pulse train $x(t)$.

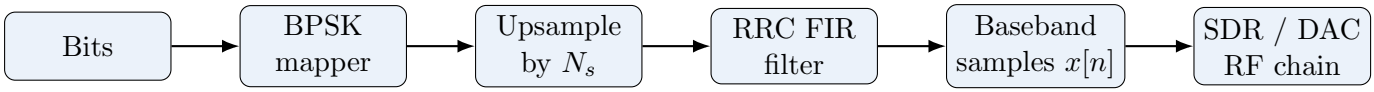


Figure 1: Digital transmitter chain for pulse-shaped BPSK.

The upsampler creates the correct sample-rate grid, and the RRC filter both interpolates between symbols and controls the occupied bandwidth.

3. Passband Transmission and Oscillator Mismatch

Suppose the RF transmitter uses carrier angular frequency ω_c. Ignoring a constant mixer normalization factor, the transmitted passband signal may be written as

$$s_{\mathrm{RF}}(t) = x(t) \cos(\omega_c t).$$

An ideal receiver would downconvert using the same carrier. In practice, the receiver local oscillator may instead be

$$\omega_c + \Delta\omega,$$

where $\Delta\omega$ is the carrier-frequency offset. The offset can arise from oscillator mismatch, Doppler shift, sampling-clock effects that appear as apparent carrier drift, or motion between transmitter and receiver.

4. How CFO Appears After I/Q Downconversion

Assume, initially, no additive noise and $r_{\mathrm{RF}}(t) = x(t) \cos(\omega_c t)$. The in-phase mixer multiplies by $\cos((\omega_c + \Delta\omega)t)$. Using

$$\cos A \cos B = \frac{1}{2}\big[\cos(A - B) + \cos(A + B)\big],$$

we obtain

$$r_{\mathrm{RF}}(t)\cos((\omega_c+\Delta\omega)t) = \frac{x(t)}{2}\left[\cos(\Delta\omega t)+\cos((2\omega_c+\Delta\omega)t)\right].$$

The low-pass filter removes the term near $2\omega_c$, leaving

$$I(t) = \frac{x(t)}{2}\cos(\Delta\omega t).$$

Similarly, the quadrature branch gives, up to the selected sine-sign convention,

$$Q(t) = \frac{x(t)}{2}\sin(\Delta\omega t).$$

In practical I/Q receivers, the factor $1/2$ is absorbed into analog or digital gain. With normalized scaling,

$$I(t) = x(t)\cos(\Delta\omega t), \qquad Q(t) = x(t)\sin(\Delta\omega t).$$

Combining the branches,

$$y_{\mathrm{BB}}(t) = I(t) + jQ(t) = x(t)e^{j\Delta\omega t}.$$

Including an unknown initial phase ϕ_0 and complex baseband noise $w(t)$ gives the fundamental CFO model

$$\boxed{y_{\mathrm{BB}}(t) = x(t)e^{j(\Delta\omega t+\phi_0)} + w(t).}$$

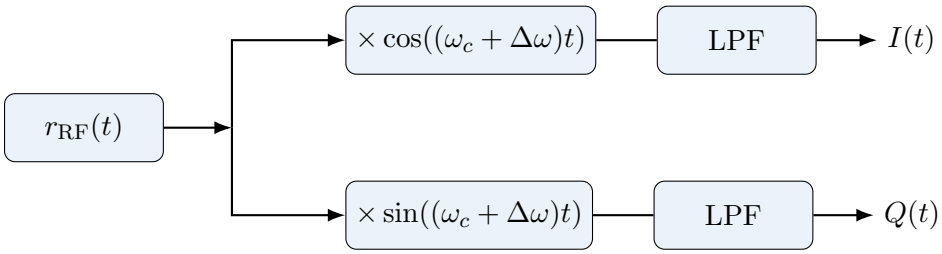


Figure 2: Quadrature downconversion with receiver oscillator offset $\Delta\omega$.

5. Interpretation: CFO Is a Linear Phase Ramp

The residual phase is

$$\theta(t) = \phi_0 + \Delta\omega t,$$

so

$$\frac{d\theta(t)}{dt} = \Delta\omega.$$

A constant CFO therefore creates a phase that changes linearly with time. In the complex plane, the constellation rotates continuously rather than suffering only a fixed angular displacement.

Sampling at $t = nT_s$ gives

$$\boxed{y[n] = x[n]e^{j(\Delta\omega nT_s+\phi_0)} + w[n].}$$

Define the normalized offset in radians/sample as

$$\boxed{\Omega = \Delta\omega T_s.}$$

Then

$$\boxed{y[n] = x[n]e^{j(\phi_0+\Omega n)} + w[n].}$$

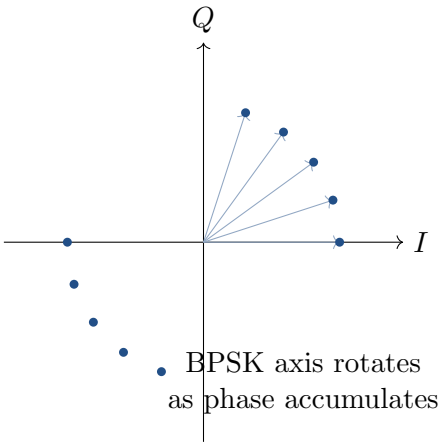


Figure 3: Residual CFO causes the BPSK constellation axis to rotate over time.

6. Why a Known Pilot Helps

With unknown data, the phase of $y[n]$ contains both modulation-dependent phase and carrier rotation. A known pilot separates the two effects. Let $x_p[n]$ be the known pilot waveform. During the pilot,

$$\boxed{y[n] = x_p[n]e^{j(\phi_0+\Omega n)} + w[n].}$$

Ignoring noise and assuming $x_p[n] \neq 0$, direct division gives

$$z[n] = \frac{y[n]}{x_p[n]} = e^{j(\phi_0+\Omega n)}.$$

This is pedagogically useful but is not the preferred implementation because division by a small pulse-shaped pilot sample can amplify noise.

A more robust construction is

$$\boxed{u[n] = y[n]x_p^*[n].}$$

Ignoring noise,

$$\boxed{u[n] = |x_p[n]|^2 e^{j(\phi_0+\Omega n)}.}$$

Thus the known modulation has disappeared; only a real positive amplitude factor and the CFO-induced phase remain.

7. Adjacent-Sample Phase-Difference Estimator

Consider adjacent pilot-compensated samples. Ignoring noise,

$$u[n+1]u^*[n] = |x_p[n+1]|^2|x_p[n]|^2 e^{j\Omega}.$$

Therefore

$$\angle\big(u[n+1]u^*[n]\big) = \Omega.$$

Averaging several such products reduces noise sensitivity:

$$R_1 = \sum_{n=0}^{N-2} u[n+1]u^*[n].$$

Because each noiseless term has the same phase Ω,

$$\boxed{\widehat{\Omega} = \angle(R_1), \qquad \widehat{\Delta\omega} = \frac{\widehat{\Omega}}{T_s}.}$$

The initial phase ϕ_0 cancels automatically in the phase difference.

8. General Lag-D Estimator

Rather than comparing adjacent samples, compare samples separated by D intervals. Ignoring noise,

$$u[n+D]u^*[n] = C_n e^{jD\Omega},$$

where $C_n \geq 0$. Define

$$R_D = \sum_n u[n+D]u^*[n].$$

Then

$$\boxed{\widehat{\Omega} = \frac{1}{D}\angle(R_D), \qquad \widehat{\Delta\omega} = \frac{1}{DT_s}\angle(R_D).}$$

A larger D produces a larger accumulated phase, which improves sensitivity to small CFO. However, phase is observed modulo 2π, so unambiguous estimation requires

$$|D\Omega| < \pi.$$

Hence the unambiguous range is

$$\boxed{|\Delta\omega| < \frac{\pi}{DT_s}.}$$

This is an important design tradeoff: increasing D improves phase sensitivity but reduces acquisition range.

9. Repeated-Preamble CFO Estimation

A common SDR preamble contains two identical blocks of length L samples. Let

$$x_p[n+L] = x_p[n].$$

The received samples satisfy approximately

$$y[n] = x_p[n]e^{j(\phi_0+\Omega n)} + w[n],$$

and

$$y[n+L] = x_p[n]e^{j(\phi_0+\Omega(n+L))} + w[n+L].$$

Ignoring noise,

$$y[n+L]y^*[n] = |x_p[n]|^2 e^{jL\Omega}.$$

Sum across the repeated block:

$$R_L = \sum_{n=0}^{L-1} y[n+L]y^*[n].$$

Then

$$\boxed{\widehat{\Omega}_{\text{coarse}} = \frac{1}{L}\angle(R_L), \qquad \widehat{\Delta\omega}_{\text{coarse}} = \frac{1}{LT_s}\angle(R_L).}$$

The transmitted waveform cancels automatically, which makes repeated-preamble estimators particularly attractive for coarse synchronization.

10. Maximum-Likelihood Pilot-Based CFO Estimation

Assume a known pilot and complex AWGN:

$$y[n] = x_p[n]e^{j(\phi+\Omega n)} + w[n].$$

The maximum-likelihood estimate minimizes squared error:

$$(\hat{\phi}, \hat{\Omega}) = \arg\min_{\phi,\Omega} \sum_n \left| y[n] - x_p[n]e^{j(\phi+\Omega n)} \right|^2.$$

For a fixed Ω, the optimum ϕ aligns the complex correlation. The frequency search therefore reduces to

$$\boxed{\hat{\Omega} = \arg\max_{\Omega} \left| \sum_n y[n]x_p^*[n]e^{-j\Omega n} \right|.}$$

Finally,

$$\boxed{\widehat{\Delta\omega} = \frac{\hat{\Omega}}{T_s}.}$$

This interpretation is useful: the correct CFO hypothesis is the one that derotates the pilot so that its samples add most coherently.

11. Digital CFO Correction

Once $\widehat{\Delta\omega}$ has been estimated, the receiver applies the opposite phase rotation. Define

$$\widehat{\Omega} = \widehat{\Delta\omega} T_s.$$

Then the corrected sample is

$$\boxed{y_c[n] = y[n]e^{-j\widehat{\Omega}n}.}$$

If $\widehat{\Delta\omega} \approx \Delta\omega$, then

$$y_c[n] \approx x[n]e^{j\phi_0} + w_c[n].$$

The continuous phase drift is removed, although a residual constant phase and a smaller residual CFO may remain.

12. NCO Implementation in an SDR

An SDR does not normally evaluate $e^{-j\widehat{\Omega}n}$ independently at every sample. Instead, a numerically controlled oscillator maintains a phase accumulator. Let $\psi[n]$ denote the NCO phase. The update is

$$\boxed{\psi[n+1] = \left(\psi[n] + \widehat{\Omega}\right) \bmod 2\pi.}$$

The NCO generates

$$c[n] = \cos\psi[n] - j\sin\psi[n],$$

and the corrected IQ sample is

$$\boxed{y_c[n] = y[n]c[n].}$$

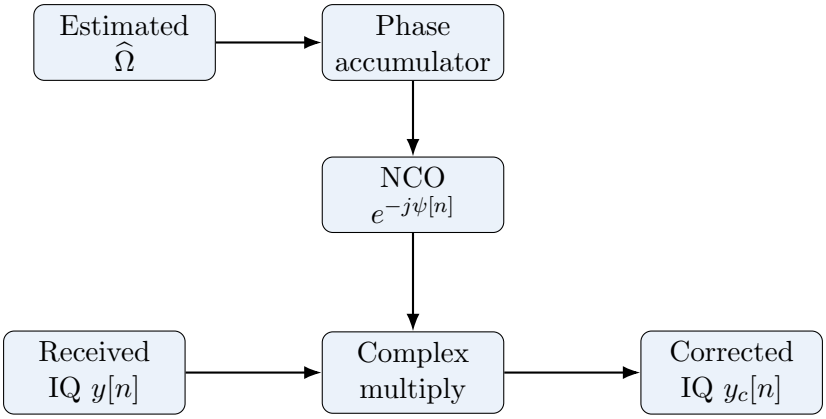


Figure 4: Digital CFO correction using an NCO and complex multiplication.

13. Where CFO Correction Sits Relative to the RRC Filter

A large CFO shifts the spectrum relative to the receive matched filter. Therefore coarse correction is preferably performed before the final matched-filter and symbol-decision stages. A practical sequence is

ADC/IQ → preamble detection → coarse CFO estimate → counter-rotation → RRC matched filter.

After matched filtering and timing recovery, a fine carrier-recovery stage removes the remaining phase and small residual frequency offset.

14. Coarse and Fine Frequency Synchronization

14.1 Coarse CFO estimation

The coarse estimator must tolerate a relatively large initial frequency uncertainty. It is commonly feedforward and preamble-based, for example using repeated blocks. Its primary goal is to move the residual CFO into the capture range of the fine tracker.

14.2 Fine carrier recovery

After coarse correction, matched filtering, and timing recovery, the symbol-rate model may be written as

$$z_k = a_k e^{j(\phi_0 + k\Delta\omega_{\text{res}} T_m)} + v_k.$$

The residual offset $\Delta\omega_{\text{res}}$ is small. Fine tracking can then use pilot phase, a decision-directed loop, or a Costas loop.

The distinction is therefore:

Stage	Main goal	Typical property
Coarse CFO	Large acquisition range	Feedforward / preamble based
Fine recovery	High precision and tracking	Feedback / decision directed

15. Costas Loop for Residual Carrier Recovery

For BPSK, suppose the symbol-rate input to the fine tracker is

$$z_k = a_k e^{j\theta_k} + v_k.$$

The Costas loop maintains a carrier-phase estimate $\hat{\theta}_k$ and counter-rotates:

$$\boxed{q_k = z_k e^{-j\hat{\theta}_k}.}$$

Write $q_k = I_k + jQ_k$. A common BPSK phase-detector error is

$$\boxed{e_k = \text{sign}(I_k)Q_k.}$$

Near lock, e_k is approximately proportional to the residual phase error $\theta_k - \hat{\theta}_k$.

A second-order digital loop tracks both residual frequency and phase. If $\hat{\Omega}_k$ is the estimated residual phase increment per symbol, then a typical update is

$$\boxed{\hat{\Omega}_{k+1} = \hat{\Omega}_k + \beta e_k,}$$

followed by

$$\boxed{\hat{\theta}_{k+1} = \hat{\theta}_k + \hat{\Omega}_{k+1} + \alpha e_k.}$$

The proportional term αe_k gives immediate phase correction, while the integral/frequency state $\hat{\Omega}_k$ learns persistent phase drift caused by residual CFO.

15.1 Control-theoretic interpretation

Near lock, model the detector as $e_k \approx K_d(\theta_k - \hat{\theta}_k)$. The Costas loop is then a nonlinear PLL operating near a stable equilibrium, and its local dynamics are those of a second-order feedback system. The NCO integrates frequency to phase, while the loop's integral path estimates the constant frequency mismatch. This is why a type-II loop can asymptotically track a constant CFO with zero steady-state phase error in the linearized model.

16. Complete Practical SDR Receiver

A useful end-to-end receiver architecture is shown below.

In an SDR, the RF transceiver typically provides complex I/Q samples to the processor or FPGA. The synchronization algorithms then operate entirely in the digital domain. Coarse CFO correction keeps the signal within the effective passband and prevents rapid constellation rotation; the RRC matched filter maximizes SNR for the chosen pulse and completes the Nyquist pulse shaping; timing recovery determines the correct symbol sampling instants; the Costas loop tracks residual carrier phase/frequency; and an equalizer is added if multipath creates significant ISI.

17. Implementation Notes

17.1 Units and normalized frequency

It is useful to distinguish three CFO quantities:

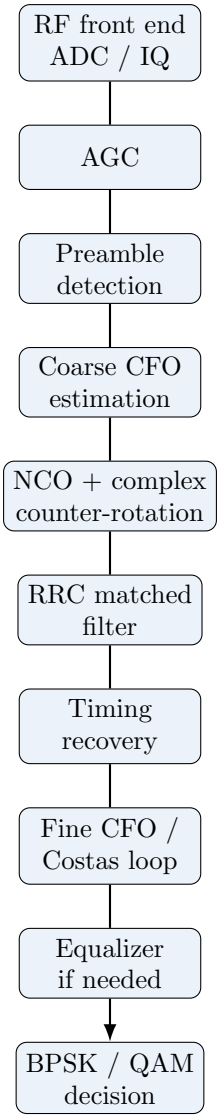


Figure 5: A practical digital synchronization chain for an SDR receiver.

- $\Delta\omega$: angular frequency offset in rad/s;
- $\Delta f = \Delta\omega/(2\pi)$: frequency offset in Hz;
- $\Omega = \Delta\omega T_s$: normalized frequency offset in rad/sample.

DSP algorithms generally operate on Ω, while RF specifications are often quoted in Hz.

17.2 Numerical example

Suppose $F_s = 1$ MHz, so $T_s = 1\,\mu$s, and the estimated normalized offset is $\hat{\Omega} = 0.02$ rad/sample. Then

$$\widehat{\Delta\omega} = \frac{0.02}{10^{-6}} = 2 \times 10^4 \text{ rad/s},$$

and

$$\widehat{\Delta f} = \frac{\widehat{\Delta\omega}}{2\pi} \approx 3.18 \text{ kHz}.$$

The NCO therefore increments its phase by 0.02 rad every sample and multiplies by the opposite complex rotation.

17.3 Residual phase after CFO correction

A one-shot CFO estimate removes the linear phase slope but usually leaves a constant phase offset and estimation error. This is why the practical architecture uses both feedforward estimation and feedback tracking rather than relying on a single estimator.

18. Summary

The main relationships are:

$$\boxed{x(t) = \sqrt{PT_m} \sum_k a_k p(t - kT_m)}$$

for pulse-shaped BPSK,

$$\boxed{y_{\mathrm{BB}}(t) = x(t)e^{j(\Delta\omega t + \phi_0)} + w(t)}$$

for continuous-time CFO,

$$\boxed{y[n] = x[n]e^{j(\phi_0 + \Omega n)} + w[n], \qquad \Omega = \Delta\omega T_s}$$

for the sampled baseband model,

$$\boxed{\widehat{\Delta\omega} = \frac{1}{DT_s} \angle \left(\sum_n u[n + D]u^*[n] \right)}$$

for a pilot-based lag-D estimator, and

$$\boxed{y_c[n] = y[n]e^{-j\widehat{\Delta\omega} n T_s}}$$

for digital CFO correction.

The practical idea is simple: a carrier-frequency mismatch becomes a linear phase drift in complex baseband. A known pilot or repeated preamble estimates the slope of that phase drift, an NCO counter-rotates the samples, and a fine carrier-recovery loop such as a Costas loop continuously tracks the remaining phase and frequency error.